View metadata, citation and similar papers at core.ac.uk
brought to you by CORE
provided by UPCommons. Portal del coneixement obert de la UPC

Algebraic Observer-Based Output-Feedback Controller Design for a PEM Fuel Cell Air-Supply Subsystem

BAROUD Zakaria[1,2,*], *GAZZAM Noureddine*[1], *BENALIA Atallah*[1], *OCAMPO-MARTINEZ Carlos*[2]

[1] *Laboratoire d'Analyse et de Commande des Systèmes d'Énergies et Réseaux Électriques. Université Amar Telidji de Laghouat, Laghouat 03000, Algérie*
[2] *Automatic Control Department, Universitat Politècnica de Catalunya, Institut de Robòtica i Informàtica Industrial (CSIC-UPC), C/ Llorens i Artigas 4-6, 08028 Barcelona, Spain*
** E-mail: z.baroud@lagh-univ.dz*

Abstract: In this paper, an algebraic-observer-based output-feedback controller is proposed for a Proton Exchange Membrane Fuel Cell (PEMFC) air-supply subsystem, based on both algebraic differentiation and sliding-mode control approaches. The goal of the design is to regulate the Oxygen Excess Ratio (OER) towards its optimal setpoint value in the PEMFC air-supply subsystem. Hence, an algebraic estimation approach is used to reconstruct the OER based on a robust differentiation method. The proposed observer is known by its finite-time convergence and low computational time compared to other observers presented in the literature. Then, a twisting controller is designed to control the OER by manipulating the compressor motor voltage. The parameters of the twisting controller have been calculated by means of an off-line tuning procedure. The performance of the proposed algebraic-observer-based output-feedback controller is analyzed through simulations for different stack-current changes, for parameter uncertainties and for noise rejection. Results show that the proposed approach properly estimates and regulates the OER in finite-time.

1 Introduction

The development of new clean energies is a major challenge of the 21^{st} century, on one hand to face environmental issues and, on the other hand, to have alternatives to fossil fuels. Hydrogen technologies, and more particularly fuel cells at low temperatures, have many advantages to be the energy generators of future. Fuel Cells are electrochemical devices that convert the chemical energy of the fuel directly into electricity, heat and water. They can be deployed in many areas such as transport, portable and stationary applications, among others [1], [2].

Among the different types of fuel cells, hydrogen Proton Exchange Membrane Fuel Cells (PEMFC) are, without doubt, the most extensively used type for transport applications [3]. This is due to their low operating temperature (typically 60-80°C), which enables fast startup. Moreover, these fuel cells have high power density, small volume, solid electrolyte, long life, as well as low corrosion [4]. However, there are still many problems to be solved before considering their development and commercialization on real systems so far. As a result, advanced control methods are required to improve their lifetime and avoid the rapid degradation of the entire PEMFC-based system [5].

This paper is interested in the control of the air-supply subsystem, which is composed of a motorized compressor (motor-compressor). In this context, many control strategies have been proposed to regulate fast and efficiently the oxygen excess ratio (OER) depleted from the fuel-cell cathode in order to avoid oxygen starvation and saturation phenomena. The last two decades have recognized the development of a significant number of control methods for the air-supply subsystem. Linear control methods based on model linearization such as Linear Quadratic Regulator (LQR), proportional integral (PI) plus static feed-forward controller and static feedback controller are presented in [6], [7], respectively. In [8], the transient behavior of the air-supply subsystem was improved using a super-twisting algorithm. In [9], fuzzy self-tuning PID controller is adopted, which is separated into two parts: fuzzy tuner and classical PID controller. An efficient controller that combines conventional PID and fuzzy logic is addressed in [10]. However, this is a challenging task because all these control strategies require knowing the exact value of OER, which depends on internal variables such as the pressure in the supply manifold and the partial pressures of both oxygen and nitrogen in the cathode. This means they should be used further sensors for measurements that increase both the overall system complexity and the cost, while decrease the efficiency of the fuel-cell system. Therefore, observers using only the measurements of available states become a cheaper and attractive solution.

Over the last few years, several studies have interested in the observer design for PEMFC systems. Some available results are recalled: from a linearized model, [11] has proposed an approach based on Kalman filter (EKF) to estimate all states of the PEMFC system. In [12], a nonlinear observer is designed by employing the derivatives of the pressures in both cathode and anode. More recently, authors in [13], [14] have presented a finite-time High-Order Sliding Mode (HOSM) observer to estimate some key states in the PEMFC air-supply subsystem. These observers are applied for the estimation of the OER in the PEMFC system with various degrees of success.

The main contribution of this work is to design an algebraic-observer-based output-feedback controller in order to estimate and regulate the OER in a PEMFC air-supply subsystem. Hence, the robustness and the accuracy of the differentiation method are important elements to the observer design. A robust differentiation method taken from [16] is adopted to estimate, in finite-time, the time derivatives of both output and input variables. The observer designed in this paper estimates the partial pressures of oxygen and nitrogen in finite-time from the measurement of the supply manifold pressure. Then, the design of the twisting controller, used in this paper as the closed-loop control strategy, is proposed where an off-line tuning procedure was used to tune the controller parameters [17], [18].

The remainder of the paper is organized as follows. The mathematical model of the PEMFC air-supply subsystem is described in Section 2. In Section 3, the problem statement and the twisting controller are outlined. The algebraic observer is designed for estimating

the OER in Section 4. Different simulation scenarios, including performance results, parameter uncertainties, noise in measurement and comparison study, are discussed in Section 5. Finally, the major conclusions are presented in Section 6.

2 PEMFC air-supply subsystem model

The PEMFC system includes five main auxiliary subsystems: the air-supply subsystem to the cathode part, the hydrogen-supply subsystem to the anode part, the stack temperature subsystem, the humidity subsystem and the stack electrochemistry subsystem. The overall PEMFC system, inputs and outputs are illustrated in Fig. 1. According to [19], it is assumed that compressed hydrogen is available. In addition, it is considered that both humidity and temperature of input reactant flows are well regulated by dedicated controllers, and thus the main attention is focused on the air-supply subsystem. Under these assumptions, a fourth-order state-space model is derived from the ninth-order model presented in [11]. The vector of states $x \in \mathbb{R}^4$ is associated to the oxygen and nitrogen partial pressures in the cathode channel, the rotational speed of the motor shaft in the compressor and the air pressure in the supply manifold, respectively. The control input $u \in \mathbb{R}$ is the compressor motor voltage $v_{cm}(t)$, which allows the manipulation of the air-supply and thus, the oxygen supply to the fuel-cell stack. The measurable disturbance input $w \in \mathbb{R}$ is the stack-current $I_{st}(t)$.

The dynamics of the oxygen and nitrogen partial pressures in the cathode channel, for the air pressure in the supply manifold and for the rotational speed of the motor shaft in the compressor are described by the following equations [20]:

$$\frac{dx_1(t)}{dt} = c_1\zeta(t) - \frac{c_3 x_1(t)\alpha(t)}{c_4 x_1(t) + c_5 x_2(t) + c_6} - c_7 w(t), \tag{1a}$$

$$\frac{dx_2(t)}{dt} = c_8\zeta(t) - \frac{c_3 x_2(t)\alpha(t)}{c_4 x_1(t) + c_5 x_2(t) + c_6}, \tag{1b}$$

$$\frac{dx_3(t)}{dt} = -c_9 x_3(t) - \frac{c_{10} y_3(t)}{x_3(t)}\left(\left(\frac{x_4(t)}{c_{14}}\right)^{c_{12}} - 1\right) + c_{13}u(t), \tag{1c}$$

$$\frac{dx_4(t)}{dt} = c_{14}\left(1 + \left(c_{15}\left(\frac{x_4(t)}{c_{11}}\right)^{c_{12}} - 1\right)\right)\left(y_3(t) - c_{16}\zeta(t)\right), \tag{1d}$$

with $\zeta(t) = x_4(t) - \chi(t) - c_2$, where constants $c_i, i \in \{1, ..., 24\}$ are defined in Table 1 in the Appendix, the air cathode pressure, $\chi(t)$, is the sum of two partial pressures, namely $x_1(t), x_2(t)$, and the equation of cathode outlet mass flow rate, $\alpha(t)$, is expressed as:

$$\alpha(t) = c_{17}(\chi(t) - c_2)\left(\frac{c_{11}}{\chi(t) - c_2}\right)^{c_{18}}\sqrt{1 - \left(\frac{c_{11}}{\chi(t) - c_2}\right)^{c_{12}}}. \tag{2}$$

The measured output $y \in \mathbb{R}^3$, as shown in Fig. 1, is the stack voltage $y_1(t) = V_{st}(t)$, the supply manifold air pressure $y_2(t) = x_4(t)$ and the compressor air mass flow rate $y_3(t) = W_{cp}(t)$, respectively. The latter is determined through the rotational speed of the motor compressor and the air pressure in the supply manifold, which has been approximated with the following expression:

$$y_3(t) = \frac{y_3^{\max} x_3(t)}{x_3^{\max}}\left(1 - e^{\lambda(t)}\right), \tag{3}$$

with

$$\lambda(t) = \frac{-r\left(s + \frac{x_3^2(t)}{q} - x_4(t)\right)}{s + \frac{x_3^2(t)}{q} - x_4^{\min}},$$

where $r = 15$, $q = 462.25$ rad^2/(s^{2}Pa), $x_3^{\max} = 11500$ rad/s, $x_4^{\min} = 50000$ Pa, $s = 100000$ Pa and $y_3^{\max} = 0.0975$ kg/s. Details on functions $y_1(t)$ and $y_3(t)$ can be found in [11], [20].

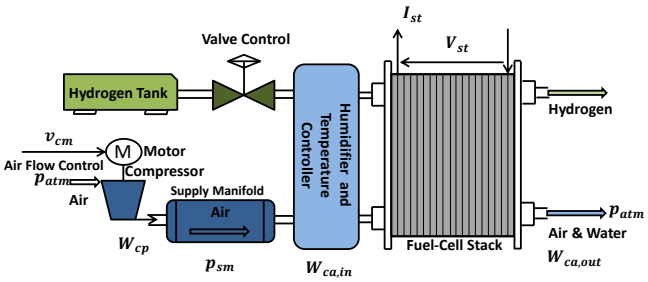

Fig. 1: The overall PEM fuel-cell system

The performance variables $z \in \mathbb{R}^2$, with $z_1(t)$ as net power and $z_2(t)$ as OER, are given as follows:

$$z_1(t) = y_1(t)w(t) - c_{21}u(t)\left(u(t) - c_{22}x_3(t)\right), \tag{4}$$

$$z_2(t) = \frac{c_{23}\left(x_4(t) - \chi(t) - c_2\right)}{c_{24}w(t)}. \tag{5}$$

3 Problem statement and controller design

3.1 Control objective

The main control objective for the PEMFC air-supply subsystem is to regulate the OER $z_2(t)$, which is defined also by the amount of oxygen provided, denoted by $W_{O_2,in}(t)$, and the amount of oxygen reacted, denoted as $W_{O_2,rct}(t)$, through the following expression:

$$z_2(t) = \frac{W_{O_2,in}(\chi(t), x_4(t))}{W_{O_2,rct}(I_{st}(t))}. \tag{6}$$

If the value of $z_2(t)$ is quite low, even though higher than 1, it is likely to cause *oxygen starvation*. This phenomenon can cause damages to the the fuel-cell membrane and degradation of the fuel-cell system efficiency. On the other hand, higher values of $z_2(t)$ will cause an excessive increase in compressor motor power and, therefore, the system net power decreased. As a result, it is necessary to state the optimal value of $z_2(t)$ that maximizes the net power $z_1(t)$. Fig. 2 shows the relation between the OER and the net power for different stack-currents, which is called the *performance curve*. This curve, for a real fuel-cell stack, is provided by the manufacturer as a part of the particular specifications of the device. It can be seen from Fig. 2 that the highest net power $z_1\,(t)$ is achieved at an OER $z_2(t)$ between 1.9 and 2.5 depending on the stack-current changes. However, in order to get the best trade-off between safety and efficiency, it is necessary to implement a controller that regulates $z_2(t)$ around an optimal value $z_{2,opt} = 2.05$ as discussed in [21].

However, according to (5), the OER depends on the internal variables that are the air pressure in the supply manifold and the partial pressures of oxygen and nitrogen in the cathode channel. Fortunately, the expression of $z_2(t)$ is related to the unknown sum of the partial pressures of oxygen and nitrogen,$\chi(t)$. Therefore, the $z_2(t)$ calculation relies only to the estimate value of $\chi(t)$. The $\chi(t)$ expression is obtained from (1d) as

$$\chi(t) = \frac{1}{c_{16}}\left(\frac{\dot{y}_2(t)}{c_{14}\left(1 + \left(c_{15}\left(\frac{y_2(t)}{c_{11}}\right)^{c_{12}} - 1\right)\right)} - y_3(t)\right) + y_2(t) - c_2. \tag{7}$$

According to (7) and to get $\chi(t)$, a robust finite-time differentiator is required to estimate the supply manifold pressure derivative. In this work, an algebraic differentiation method, presented in [23], will

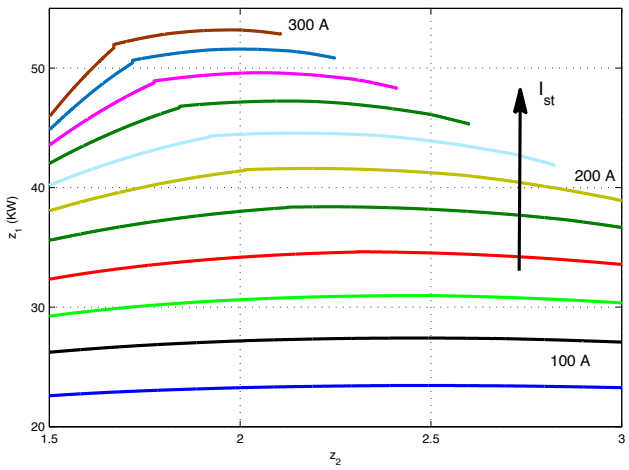

Fig. 2: Fuel-cell system performance under different stack-currents

be designed in order to maintain the following condition:

$$e(t) = \hat{\chi}(t) - \chi(t) = 0 \qquad \forall \quad t \geq T, \quad T \in \mathbb{R}^{+}, \tag{8}$$

where T is a positive constant, which is chosen to improve the precision of the estimated derivative, $\hat{\dot{y}}_2(t)$. The estimate value of OER, $\hat{z}_2(t)$, can be obtained for some finite $T > 0$ according to

$$\hat{z}_2(t) = \rho(t)\left(y_2(t) - \hat{\chi}(t) - c_2\right), \tag{9}$$

with $\rho(t) = \frac{c_{23}}{c_{24}w(t)}$. It is important to notice that the algebraic observer converges in finite time, then the separation principle of observation and control can be fixed as in [14]. Thus, the feedback controller using the estimated OER (9) can be designed separately from the algebraic observer. Besides, define the corresponding regulation-error variable as

$$\hat{\sigma}(t) = \hat{z}_2(t) - z_{2,opt}, \tag{10}$$

which will be driven to zero in finite time and will be kept at zero thereafter by a suitable twisting controller whose design is given below.

3.2 Twisting controller

Collecting (1) in a unique state-space representation, yields the form

$$\begin{aligned}\dot{x}(t) &= f(x(t)) + gu(t) + \varphi w(t),\\ &= \begin{bmatrix} f_1(x_1,x_2,x_4)\\ f_2(x_1,x_2,x_4)\\ f_3(x_3,x_4)\\ f_4(x_1,x_2,x_3,x_4)\end{bmatrix} + \begin{bmatrix}0\\0\\c_{13}\\0\end{bmatrix} u(t) - \begin{bmatrix}-c_7\\0\\0\\0\end{bmatrix} w(t),\end{aligned} \tag{11}$$

where $f_i : \mathbb{R}^4 \mapsto \mathbb{R}^4$, $i = \{1, \ldots, 4\}$, are smooth state maps. Considering the regulation error variable (10) as the sliding variable, the control problem for the PEMFC air-supply subsystem can be mathematically formulated as follows:

$$\begin{cases} \dot{x}(t) = f(x(t)) + gu(t) + \varphi w(t),\\ \hat{\sigma}(t) \in \mathbb{R}, \end{cases} \tag{12}$$

with a bounded control action $u(t) \in \mathbb{R}$, the measurable disturbance $w(t) \in \mathbb{R}$ is a piece-wise constant function, and $\hat{\sigma}(t)$ is a smooth function.

Note that the sliding variable expressed in (10) can be rewritten as

$$\hat{\sigma}(t) = \rho(t)\Lambda\hat{x}(t) - \rho(t)(c_2 - z_{2,opt}). \tag{13}$$

being $\Lambda = [-1 \quad -1 \quad 0 \quad 1]$. Differentiating twice the sliding variable with respect to time, the following expressions are obtained:

$$\begin{aligned}\dot{\hat{\sigma}}(t) &= \rho(t)\Lambda\dot{\hat{x}}(t),\\ &= \rho(t)\Lambda\left(f(\hat{x}(t)) + gu(t) + \varphi w(t)\right),\\ &= \rho(t)\Lambda\left(f(\hat{x}(t)) + \varphi w(t)\right),\end{aligned} \tag{14}$$

and

$$\begin{aligned}\ddot{\hat{\sigma}}(t) &= \frac{\partial\dot{\hat{\sigma}}}{\partial\hat{x}}\dot{\hat{x}}(t),\\ &= \rho(t)\Lambda\Big[\frac{\partial f\left(\hat{x}(t)\right)}{\partial\hat{x}}\left(f(\hat{x}(t)) + gu(t) + \varphi w(t)\right)\Big],\\ &= \Psi\left(\hat{x}(t), w(t)\right) + \Phi(\hat{x}(t))u(t),\end{aligned} \tag{15}$$

with

$$\Psi\left(\hat{x}(t), w(t)\right) = \rho(t)\Lambda\Big[\frac{\partial f\left(\hat{x}(t)\right)}{\partial\hat{x}}\left(f(\hat{x}(t)) + \varphi w(t)\right)\Big], \tag{16a}$$

$$\begin{aligned}\Phi(\hat{x}(t)) &= \rho(t)\Lambda\frac{\partial f\left(\hat{x}(t)\right)}{\partial\hat{x}}g,\\ &= \rho(t)\frac{\partial f_4}{\partial x_3}.\end{aligned} \tag{16b}$$

Functions $\Psi\left(\hat{x}(t), w(t)\right)$ and $\Phi(\hat{x}(t))$ can be bounded as follows:

$$\left|\Psi\left(\hat{x}(t), w(t)\right)\right| \leq \Theta, \tag{17a}$$

$$0 < B_m \leq \Phi(\hat{x}(t)) \leq B_M. \tag{17b}$$

The bounding values Θ, B_m and B_M were computed by means of a numerical study of functions $\Psi\left(\hat{x}(t), w(t)\right)$ and $\Phi(\hat{x}(t))$. After calcuation, the following bounding values can be obtained:

$$\Theta = 3 \times 10^5, \quad B_m = 450, \quad B_M = 475. \tag{18}$$

Once bounds in (18) have been determined, the stabilisation problem of system (12) with sliding variable dynamics (15) can be solved through the stabilisation of the following equivalent differential inclusion by applying twisting algorithm:

$$\ddot{\hat{\sigma}}(t) \in [-\Theta,\ \Theta] + [B_m,\ B_M]u(t). \tag{19}$$

The algorithm structure and the chosen parameters for the PEMFC air-supply subsystem controller are recalled below. The resultant control law related to the twisting algorithm is defined by [17]

$$u(t) = -(r_1\text{sign}(\hat{\sigma}(t)) + r_2\text{sign}(\dot{\hat{\sigma}}(t))), \tag{20}$$

where r_1 and r_2 are design parameters that were derived from the corresponding sufficient conditions for finite-time convergence of the algorithm [21]. Note that the derivative of the sliding variable, $\dot{\hat{\sigma}}(t)$, is estimated also through an algebraic differentiator similar to $\hat{\dot{y}}_2(t)$ in (24).

Theorem 1. *(Taken from [17]) Let r_1 and r_2 satisfy the conditions*

$$\begin{cases} r_1 > r_2 > 0,\\ (r_1 + r_2)B_m - \Theta > (r_1 - r_2)B_M + \Theta,\\ (r_1 - r_2)B_m > \Theta. \end{cases} \tag{21}$$

The controller in (20) guarantees the appearance of second-sliding-mode $\hat{\sigma}(t) = \dot{\hat{\sigma}}(t) = 0$ attracting the trajectory of the sliding variable dynamics (15) in finite-time.

Proof: The proof follows from [17]. □

Through the set of parameters that satisfy (16), the control parameters are chosen as:

$$r_1 = 750, \qquad r_2 = 0.1. \tag{22}$$

4 Algebraic observer design for PEMFC air-supply subsystem model

In this section, an algebraic observer is developed for estimating the OER from the measurement of supply manifold pressure. The proposed observer is known for its low computational time, and its finite-time convergence and its robustness against measurement noise compared to other observers presented in the literature [16]. However, before designing the observer, the algebraic observability of the PEMFC air-supply subsystem should be verified. Liu et al. [22] demonstrated that the PEMFC air-supply subsystem is algebraically observable, which means that all the system states can be expressed in terms of input and output variables, and their time derivatives up to some finite number. Hence, the implementation of the algebraic observer needs an exact numerical differentiation of input and output variables.

From (20), the twisting controller requires only the estimated value of oxygen and nitrogen partial pressures at the cathode channel (i.e., the expression $\chi(t) = x_1(t) + x_2(t)$). Estimation of $\chi(t)$ makes possible the computation of the OER, $z_2(t)$, through (5). Moreover, the value of $\chi(t)$ can be calculated using only the first derivative of the supply manifold pressure $y_2(t)$ in (1d) and the measured output $y_3(t)$ in (3). As considered in Section 2, the supply manifold pressure is measurable and its finite-time derivative is estimated by employing the robust numerical differentiation method detailed in [16].

The work reported in [15] provides the robust computation of the output derivative $y_2(t)$ based on the truncated Taylor expansion of $y_2(t)$ around time t' as follows:

$$y_2(t) = y_2^{(0)}(t') + y_2^{(1)}(t')(t - t'). \tag{23}$$

This identification procedure consists in several algebraic manipulations on the operational Laplace domain [16]. From [23], the first-order derivative estimation of the supply manifold pressure is given as follows:

$$\hat{y}_2(t) = \int_0^T \frac{6}{T^3}\left(2T - 3\tau\right) Y\left(t - \tau\right) d\tau, \tag{24}$$

where $Y(t)$ represents the noisy supply manifold pressure measurement. Then, it can be obtain robustly $\hat{\chi}(t)$ from (1d) and (24) as follows:

$$\hat{\chi}(t) = \frac{1}{c_{16}}\left(\frac{\hat{\dot{y}}_2(t)}{c_{14}\left(1 + \left(c_{15}\left(\frac{x_4(t)}{c_{11}}\right)^{c_{12}} - 1\right)\right)} - y_3(t)\right) + x_4(t) - c_2. \tag{25}$$

Depending on the response time of the system, a relevant sliding time window, T, is chosen in order to obtain an accurate value of $\dot{x}_4(t)$, and thus the estimated states $\hat{\chi}(t)$ reach the real states, $\chi(t) = x_1(t) + x_2(t)$, i.e.,

$$\hat{\chi}(t) = \chi(t). \tag{26}$$

The proposed observer/controller is schematically shown in Fig. 3, where $\hat{z}_2(t)$ is estimated using the expression provided by the algebraic observer $\hat{\chi}(t)$ and the nominal PEMFC parameters, defined in Table 2 into the Appendix, according to the following expression:

$$\hat{z}_2(t) = \zeta(t)\rho(t). \tag{27}$$

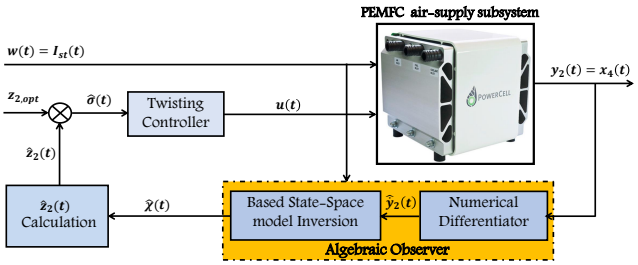

Fig. 3: Algebraic observer-based output-feedback control for a PEMFC air-supply subsystem

Remark 1. *It is worth to remark that the algebraic observer is able to reconstruct the OER in finite-time. Therefore, the separation principle is automatically satisfied and the twisting controller and the algebraic observer can be separately designed. Moreover, the stability of the closed-loop system is guaranteed because the differential inclusion* (19) *is satisfied due to the twisting algorithm [12].*

5 Simulation results

The proposed observer-based control strategy is applied to the model of the PEMFC air-supply susbsystem in (1). To assess the performance, the effectiveness and the robustness of the proposed observer-based control strategy, detailed simulations are peformed and analysed. Simulation are divided into four scenarios: nominal performance, parameter uncertainty, noise rejection and comparison study. The numerical parameters for simulation are based on a fuel-cell prototype vehicle, which corresponds to a 75 kW high-pressure FC stack fed by a 14 kW turbo compressor used in a Ford P2000 FC electric vehicle [24]. The numerical parameters are given in Table 2 in the Appendix. All the simulation have been performed using the Matlab/Simulink environnement. The initial values of the states are

$$x(0) = \left[\begin{array}{cccc} 11004\,\text{Pa} & 83813\,\text{Pa} & 5200\,\text{rad/s} & 149000\,\text{Pa} \end{array}\right]^T.$$

Note that the main aim of the proposed observer-based control strategy is to estimate/regulate the OER, $\hat{z}_2(t)$, at an optimal setpoint value by means of compressor motor voltage v_{cm} (t). With this optimal setpoint, which is set equal to 2.05, it can be assured that the PEMFC air-supply subsystem achieves the maximum net power during stack-current variation while the oxygen starvation is avoided.

The stack-current, i.e. the load is shown in Fig. 4, steps up from 100 A to 150 A at t=5 s. Next, after 5 s, it rises up by 50 A. This increment stopped when the stack-current reaches 250 A. After 20 s, the current decreases to 220 A. Finally, at time t=25 s, it increases again from 220 A to 250 A. This stack-current behaviour is adopted for all simulation scenarios.

5.1 Scenario 1. Nominal Performance

This scenario focuses on the performance of the closed-loop system by showing the actual and the estimated value of OER. No parameter uncertainty and no noise in the supply manifold pressure are considered in this scenario.

Fig. 5(b) shows that the value of OER is estimated in finite-time by the proposed algebraic observer. Fig. 5(a) presents both the real and estimated values of oxygen and nitrogen partial pressures. These partial pressures are properly estimated based on the algebraic observer. In the beginning of the estimation, the proposed observer reached the real value of $\chi(t)$ in less than 30 ms. The real and the estimated values of OER are shown in Fig. 5(b). As can be seen from Fig. 5(c), the estimation error is acceptably low in spite of having a stack-current variation. The dynamic behaviour of actual and estimated OER under different stack-current variation are illustrated in Fig. 5(b). In conclusion, the proposed observer-based control scheme

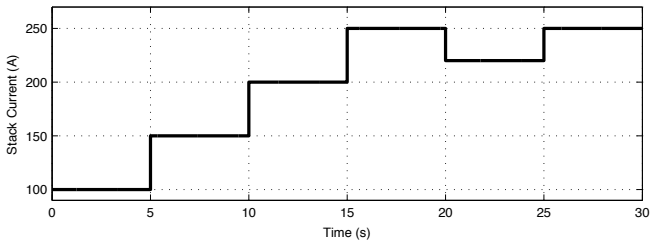

Fig. 4: Stack current variation

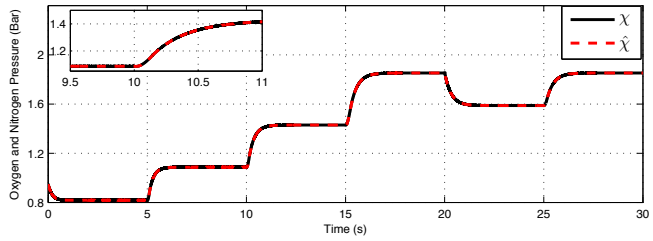

(a)

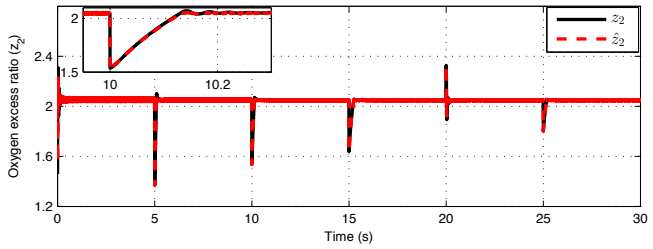

(b)

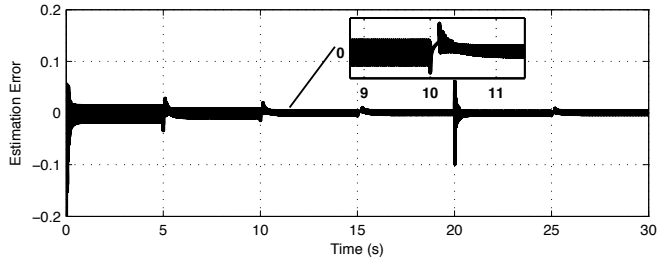

(c)

Fig. 5: Scenario 1: Performance Results
(a). Real and estimated values of oxygen and nitrogen partial pressures
(b). Real and estimated values of OER
(c). Estimation error $(z_2 - \hat{z}_2)$

Table 1 Variation of system parameters

Parameter	Nominal value	Variation
Stack temperature T_{st} [K]	353.15	$+10\,\%$
Atmospheric temperature T_{atm} [K]	298.15	$+10\,\%$
Supply manifold volume V_{sm} [m^3]	0.02	$-10\,\%$
Compressor inertia J_{cp} [kg m^{-2}]	5×10^{-5}	$+10\,\%$

adjusts $\hat{z}_2(t)$ suitably and accurately at the setpoint $z_{2,opt}$ in the presence of $I_{st}(t)$ variation.

5.2 Scenario 2. Parameter uncertainties

This scenario focuses on the effect of some parameter uncertainties in the performance of the algebraic-observer-based output-feedback controller. The variation of system parameters is listed in Table 1 [21].

Fig. 6(a) shows the real and the estimated values of oxygen and nitrogen partial pressures. Fig. 6(a) indicates the favorable robust performance of the proposed observer-based control scheme in the face of the parameter uncertainties and disturbance variation. In addition, Fig. 6(b) shows that the OER is estimated and regulated with sufficient accuracy. The proposed observer-based control remains the estimation error $(z_2 - \hat{z}_2)$, shown in Fig. 6(c), into an acceptable range during this scenario. The outputs, stack voltage and net power of the PEMFC air-supply subsystem are depicted in Figs. (6(d), 6(e)), respectively. It can be seen from these figures that, during a positive stack-current step, the stack voltage drops due to the decreasing of oxygen concentration in the cathode channel. This fact, in turn, causes an important increase in the net power.

5.3 Scenario 3. Noise rejection

In this scenario, some simulations were carried out to test the robustness of the proposed observer-based control scheme in the presence of noise in the supply manifold pressure $y_2(t)$. Let $Y(t) = y_2(t) + \xi(t)$ be the real measurement of y_2, where $\xi(t)$ is a noisy signal with mean $\mu = 3.11 \times 10^{-3}$ and variance $\sigma^2 = 4.00948$.

The simulation results are shown in Fig. 7(a) and 7(b). The real and estimated values of the OER are depicted in Fig. 7(b). In that figure, it is possible to look that the proposed observer-based control scheme both estimates and regulates the OER well enough in spite of the noise in the measurement of the supply manifold pressure.

5.4 Scenario 4. Comparison study

Here, a comparison study between the proposed observer-based control scheme and one of the recent observer-based control architectures published in the literature for the same control objective. The authors in [14] have presented an observer-based control scheme for estimating and regulating the OER of PEMFC air-supply subsystem around an optimal value, $z_{2,opt} = 2.06$. Firstly, the nonlinear observer design is based on high-order sliding algorithms. Secondly, the control loop, which uses the observed OER ($\hat{z}_2$), is also based on the HOSM and its parameters are tuned by using local linearization and frequency domain arguments [14].

Simulations of the observer-based control scheme are performed including the same stack-current demand adopted in [14], which is shown in Fig. 8(a). Fig. 8(b) shows the actual and the estimated profiles of oxygen and nitrogen partial pressures. According to Fig. 8(b), it can be seen the precision of the algebraic observer. Fig. 8(c) presents the actual and the estimated value of OER. Suitable transient response and proper estimation are shown despite large load variations. Fig. 8(c) exhibits also the zoomed plot of z_2 at t=35 s, where the proposed observer-based controller has improved greatly the transient response of $\hat{z}_2$ compared to the observer-based control strategy presented in [14] (see Fig. 8(d)).

6 Conclusions

In this article, an algebraic-observer-based output-feedback controller has been designed for regulating the oxygen excess ratio of a Proton Exchange Membrane Fuel Cell air-supply subsystem at an optimal setpoint value. The algebraic observer design provides a finite-time converging oxygen excess ratio reconstruction based on a robust differentiation method. The proposed controller, which uses the estimated oxygen excess ratio, is based on one of the second-order sliding-mode variety algorithms. This paper used the twisting algorithm depending only on few parameters, which were calculated during an off-line tuning procedure. Four simulation scenarios have shown that the designed algebraic-observer-based output-feedback controller is robust to external disturbances, parameter uncertainties and measurement noise. In the future, the proposed observer-based control scheme will be applied in an experimental test bench.

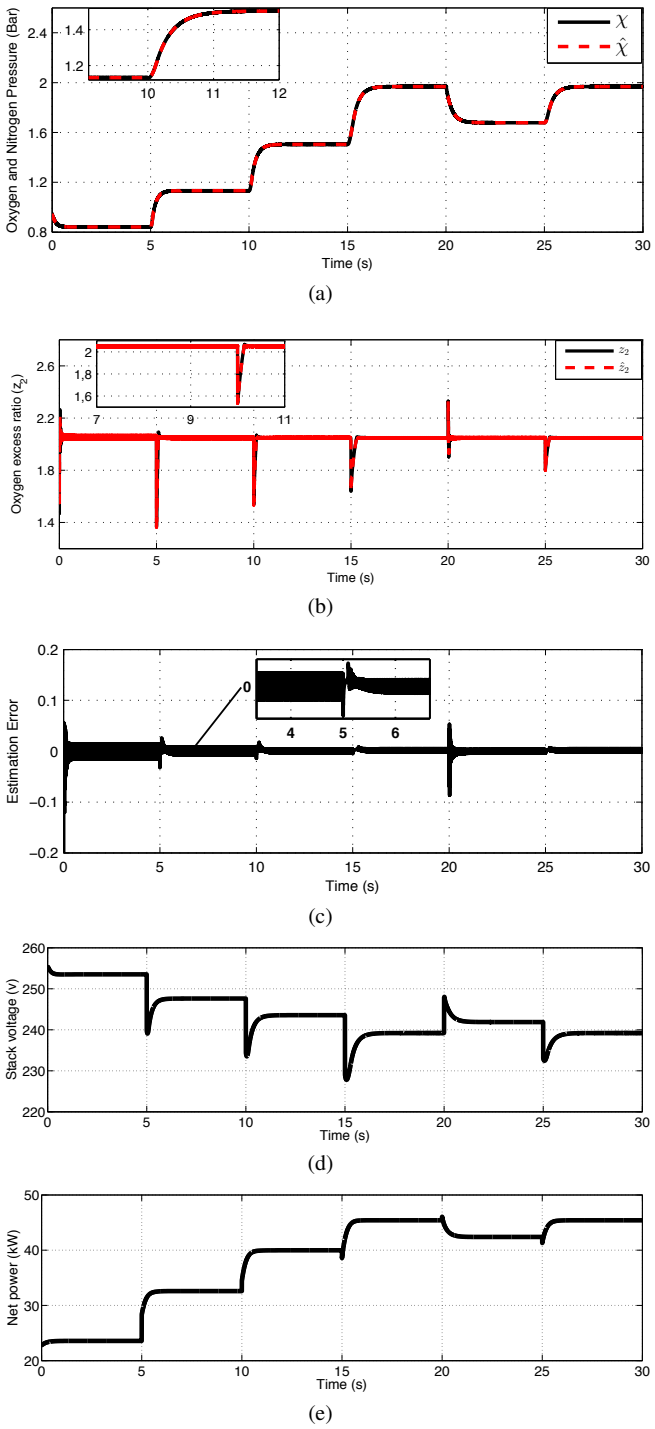

Fig. 6: Scenario 2: Parameter Uncertainties
(a). Real and estimated values of oxygen and nitrogen partial pressures
(b). Real and estimated values of OER
(c). Estimation error $(z_2 - \hat{z}_2)$
(d). Output stack voltage
(e). Output net power

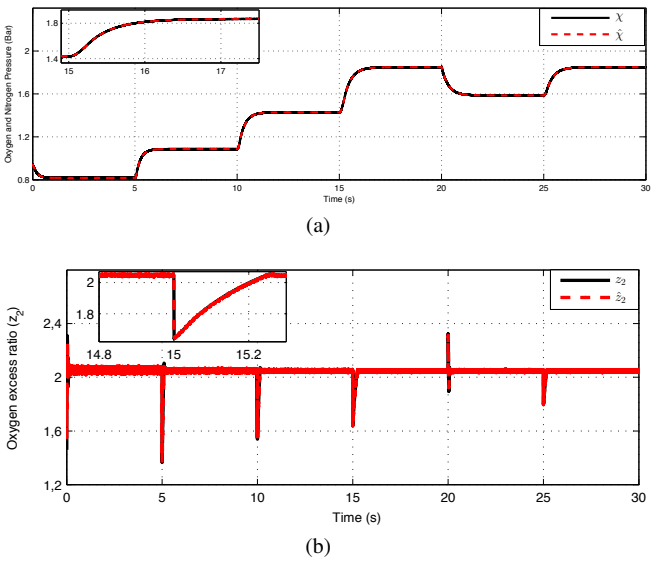

Fig. 7: Scenario 3: Noise Rejection
(a). Real and estimated values of oxygen and nitrogen partial pressures
(b). Real and estimated values of OER

Acknowledgement

This work was supported by Laboratoire d'Analyse et de Commande des Systèmes d'Énergies et Réseaux Électriques. Université Amar Telidji de Laghouat, Laghouat 03000, Algérie. The work of C. Ocampo-Martinez is partially supported by the project DEOCS (Ref. DPI2016-76493-C3-3-R) from the Spanish MINECO/FEDER.

References

[1] Ludwig J., Jürgen G.:'Polymer Electrolyte Membrane Fuel Cells', in Töpler J., Lehmann J. (Ed.):'Hydrogen and Fuel Cell: Technologies and Market Perspectives' (Springer Berlin Heidelberg, 2016, 1st edn.), pp. 239–281

[2] Boscaino V., Capponi G., Miceli R., Galluzzo G.R., Rizzo R.: 'Comparison of models of fuel cells based on experimental data for the design of power electronics systems', *IET Renewable Power Generation*, 2015, 6 (**9**), pp. 660–668

[3] Larminie J., Dicks A.: 'Proton Exchange Membrane Fuel Cells', in Wiley: 'Fuel cell systems explained' (Wiley, 2003, 2nd edn.), pp. 155–175

[4] Baroud Z., Benmiloud M., Benalia A., Ocampo-Martinez C.: 'Novel hybrid fuzzy-PID control scheme for air supply in PEM fuel cell-based systems', *International Journal of Hydrogen Energy*, 2017, 42 (**15**), pp. 10435–10447

[5] Wang M.H., Huang M., Jiang W., Liou K.: 'Maximum power point tracking control method for proton exchange membrane fuel cell', *IET Renewable Power Generation*, 2016, 7 (**10**), pp. 908–915

[6] Niknezhadi A., Allué-Fantova M., Kunusch C., Ocampo-Martinez C.: 'Design and implementation of LQR/LQG strategies for oxygen stoichiometry control in PEM fuel cells based systems', *Journal of Power Sources*, 2011, 196 (**9**), pp. 4277–4282

[7] Pukrushpan J.T., Stefanopoulou A., Peng H.: 'Control of fuel cell breathing', *IEEE Control Systems Magazine*, 2004, 42 (**2**), pp. 30–46

[8] Baroud Z., Benmiloud M., Benalia A.: 'Sliding mode controller for breathing subsystem on a PEM fuel cell system'. Proc. Int. Conf. on Control and Engineering Information Technology, Tlemcen, Algeria, May 2015, pp. 1–6

[9] Baroud Z., Benmiloud M., Benalia A.: 'Fuzzy self-tuning PID controller for air supply on a PEM fuel cell system'. Proc. Int. Conf. on Electrical Engineering, Boumerdes, Algeria, November 2015, pp. 1–4

[10] Baroud Z., Benalia A., Ocampo-Martinez C.: 'Air Flow Regulation in Fuel Cells: An Efficient Design of Hybrid Fuzzy-PID Control', *Electrotehnica, Electronica, Automatica (EEA)*, 2016, 64 (**4**), pp. 28–32

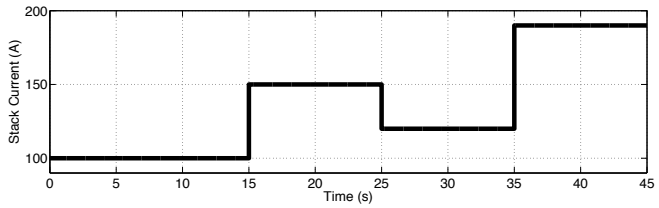

(a)

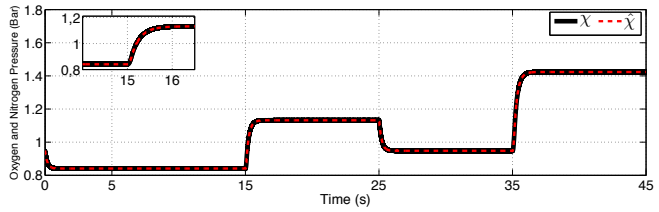

(b)

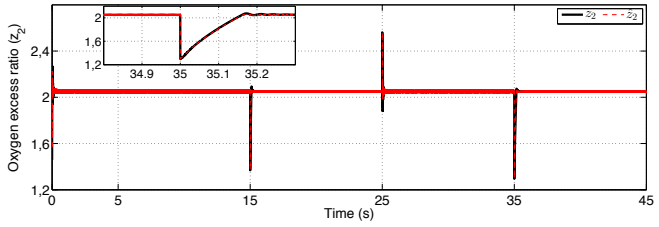

(c)

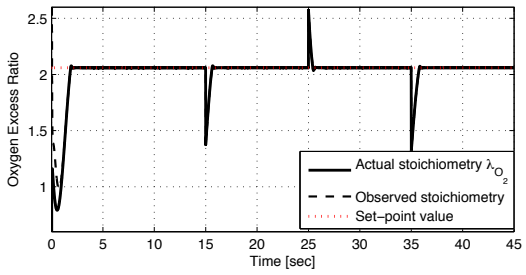

(d)

Fig. 8: Scenario 4: Comparison Study
(a). Pilloni et al. [14] stack-current variation
(b). Real and estimated values of oxygen and nitrogen partial pressures
(c). Real and estimated values of OER
(d). Real and estimated values of OER (Pilloni et al.[14])

[11] Pukrushpan J.T., Stefanopoulou A., Peng H.: 'Fuel Cell System Model: Fuel Cell Stack', in Springer: 'Control of Fuel Cell Power Systems', (Springer, 2004, 1st edn.)

[12] Kim E.: 'Observer Based Nonlinear State Feedback Control of PEM Fuel Cell Systems', *Journal of Electrical Engineering & Technology*, 2012, 7 (**6**), pp. 891–897

[13] Rakhtala S.M., Noei A.R., Ghaderi R., Usai E.: 'Design of finite-time high-order sliding mode state observer: A practical insight to PEM fuel cell system', *Journal of Process Control*, 2014, 24 (**1**), pp. 203–224

[14] Pilloni A., Pisano A., Usai E.: 'Observer-Based Air Excess Ratio Control of a PEM Fuel Cell System via High-Order Sliding Mode', *IEEE Transactions on Industrial Electronics*, 2015, 62 (**8**), pp. 5236–5246

[15] Baroud Z., Gazzam N., Benalia A.: 'Algebraic Observer Design for PEM Fuel Cell System'. Proc. Int. Conf. on Modelling, Identification and Control, Algiers, Algeria, November 2016, pp. 1–5

[16] Fliess, M., Sire-Ramirez, H.J.:'Control via state estimations of some nonlinear systems'.Proc. IFAC Symposium on Nonlinear Control Systems (NOLCOS), Stuttgart, Germany, September 2004, pp. 1121-1126

[17] Shtessel Y., Christopher E., Leonid F., Arie L.: 'Higher-Order Sliding Mode Controllers and Differentiators', in Springer Berlin Heidelberg: 'Sliding mode control and observation', (Springer, 2014, 1st edn.), pp. 213–249

[18] Fridman L., Barbot J.P., Plestan J.: 'Recent Trends in Sliding Mode Control' (Institution of Engineering and Technology, U.K., 2016, 1st edn.)

[19] Suh K.W.:'Modeling, analysis and control of fuel cell hybrid power systems', PhD thesis, Michigan University, 2006

[20] Gruber J., Bordons C., Dorado F.: 'Nonlinear control of the air feed of a fuel cell'. Proc. American Control Conf., Seattle, Washington, US, June 2008, pp. 1–6

[21] Kunusch C., Puleston P., Mayosky M.:'Control-Oriented Modelling and Experimental Validation of a PEMFC Generation System', in Kunusch, C., et al. (Ed.):'Sliding-Mode Control of PEM Fuel Cells' (Springer-Verlag London, 2012, 1st edn.), pp. 105–128

[22] Liu J., Laghrouche S., Ahmed Z.S., Wack M.: 'PEM fuel cell air-feed system observer design for automotive applications: An adaptive numerical differentiation approach', *International Journal of Hydrogen Energy*, 2014, 39 (**30**), pp. 17210 – 17221

[23] Mboup M., Join C., Fliess M.:'A revised look at numerical differentiation with an application to nonlinear feedback control'.Proc. 15th Mediterrean Conference on Control and Automation-MED, Athènes, Greece, Jun 2007, pp. 1–6

[24] Baroud Z., Benalia, A., Ocampo-Martinez, C.: 'Robust fuzzy sliding mode control for air supply on PEM fuel cell system', *Int. J. Modelling, Identification and Control*, 2018, 29 (**4**), pp. 341 – 351

Appendices

Constants and Parameters of the PEMFC air-supply subsystem model

Table 1 Constants of the PEMFC air-supply subsystem model

$c_1 = \frac{RT_{st}k_{sm,out}}{M_{O_2}V_{ca}}\left(\frac{x_{O_2,atm}}{1+\omega_{atm}}\right)$	$c_{15} = \frac{1}{\eta_{cp}}$
$c_2 = p_{sat}$	$c_{16} = k_{sm,out}$
$c_3 = \frac{RT_{st}}{V_{ca}}$	$c_{17} = \frac{C_D A_T}{\sqrt{RT_{st}}}\sqrt{\frac{2\gamma}{\gamma-1}}$
$c_4 = M_{O_2}$	$c_{18} = \frac{1}{\gamma}$
$c_5 = M_{N_2}$	$c_{19} = \left(\frac{2}{\gamma+1}\right)^{\frac{\gamma}{\gamma-1}}$
$c_6 = M_v p_{sat}$	$c_{20} = \frac{C_D A_T}{\sqrt{RT_{st}}}\gamma^{0.5}\left(\frac{2}{\gamma+1}\right)^{\frac{\gamma+1}{2\gamma-2}}$
$c_7 = \frac{RT_{st}n}{4FV_{ca}}$	$c_{21} = \frac{1}{R_{cm}}$
$c_8 = \frac{RT_{st}k_{sm,out}}{M_{N_2}V_{ca}}\left(\frac{1-x_{O_2,atm}}{1+\omega_{atm}}\right)$	$c_{22} = k_v$
$c_9 = \frac{\eta_{cm}k_t k_v}{J_{cp}R_{cm}}$	$c_{23} = k_{sm,out}\left(\frac{x_{O_2,atm}}{1+\omega_{atm}}\right)$
$c_{10} = \frac{C_p T_{atm}}{J_{cp}\eta_{cp}}$	$c_{24} = \frac{nM_{O_2}}{4F}$
$c_{11} = p_{atm}$	$x_{O_2,atm} = \frac{y_{O_2,atm}M_{O_2}}{M_{a,atm}}$
$c_{12} = \frac{\gamma-1}{\gamma}$	$\omega_{atm} = \frac{M_v}{M_{a,atm}}\frac{\phi_{atm}p_{sat}}{p_{atm}-\phi_{atm}p_{sat}}$
$c_{13} = \frac{\eta_{cm}k_t}{J_{cp}R_{cm}}$	
$c_{14} = \frac{RT_{atm}\gamma}{M_{a,atm}V_{sm}}$	

Table 2 Simulation Parameters

Parameter	Description	Value	Unit
η_{cp}	Motor mechanical efficiency	0.98	%
η_{cm}	Compressor efficiency	0.8	%
J_{cp}	Compressor inertia	5×10^{-5}	kg m^{-}2
R_{cm}	Compressor motor resistance	0.82	Ω
k_t	Motor parameter	0.0153	(N m)/A
k_v	Motor parameter	0.0153	V/(rad/s)
$M_{a,atm}$	Air molar mass	29×10^{-3}	kg mol^{-1}
M_{O_2}	Oxygen molar mass	32×10^{-3}	kg mol^{-1}
M_{N_2}	Nitrogen molar mass	28×10^{-3}	kg mol^{-1}
M_v	Vapor molar mass	18×10^{-3}	kg mol^{-1}
$y_{O_2,atm}$	Oxygen mole fraction	0.21	–
V_{ca}	Cathode volume	0.01	m^3
$k_{sm,out}$	Supply manifold outlet orifice constant	0.3629×10^{-5}	kg/(s Pa)
V_{sm}	Supply manifold volume	0.02	m^3
T_{st}	Stack temperature	353.15	K
T_{atm}	Atmospheric temperature	298.15	K
p_{atm}	Atmospheric pressure	101325	Pa
p_{sat}	Saturation pressure	465327.41	Pa
R	Universal gas constant	8.3145	J/(mol K)
C_p	Constant pressure Specific heat of air	1004	J/(mol K)
C_D	Cathode outlet throttle discharge coefficient	0.0124	–
γ	Ratio of specific heat of air	1.4	–
A_T	Cathode outlet throttle area	0.002	m^2
ϕ_{atm}	Average ambient air relative humidity	0.5	–
n	Number of cells in fuel-cell stack	381	–
F	Faraday number	96485	C mol^{-1}